

Medical Image Fusion Schemes using Contourlet Transform and PCA Based

Nemir Al-Azzawi and Wan Ahmed K. Wan Abdullah
*Biomedical Electronics group, Universiti Sains Malaysia
Penang,
Malaysia*

1. Introduction

Fusion imaging is one of the most modern, accurate and useful diagnostic techniques in medical imaging today. The new technology has made a clear difference in patient care by compressing the time between diagnosis and treatment. Although image fusion can have different purposes, the main aim of fusion is spatial resolution enhancement or image sharpening. Also known as integrated imaging, it provides a computer link that allows for the combination of multimodal medical images into a single image with more complete and accurate description of the same object. The benefits are even more profound in combining anatomical imaging modalities with functional ones. For example, PET-CT in lung cancer, MRI-PET in brain tumors, SPECT-CT in abdominal studies and ultrasound images-MRI for vascular blood flow (Patias, 2002). Outcome of MRI-CT image fusion has been shown to be able to assist in planning surgical procedure. Mainly, medical image fusion try to solve the issue of where there is no single modality provides both anatomical and functional information. Further more information provided by different modalities may be in agreement or in complementary nature.

An important research issue in medical image processing, specifically in information computation, is fusion of multimodal information (Daneshvar and Ghassemian, 2007; Hong *et al.*, 2007; Zhongfei *et al.*, 2003). Existing algorithms generally use discrete wavelet transform (DWT) (Anna *et al.*, 2007; Pajares and Manuel de la Cruz, 2004; Singh *et al.*, 2009) for multimodal medical image fusion because DWT preserves different frequency information in stable form and allows good localization both in time and spatial frequency domain. However, one of the major drawbacks of DWT is that the transformation does not provide shift invariance.

This causes a major change in the wavelet coefficients of the image even for minor shifts in the input image. In medical imaging, it is important to know and preserve the exact location of this information, but shift variance may lead to inaccuracies. As an alternative (Kingsbury, 1999), proposed dual-tree complex wavelet transform (DT-CWT) which provides approximate shift invariance. DT-CWT has the drawback of limited directional information. Hence, contourlet transform was proposed to capture the most important salient information in images by incorporating the DT-CWT and DFB (Chen and Li, 2005).

Extensive researches have been conducted on image fusion techniques, and various fusion algorithms for medical image have been developed depending on the merging stage (Aguilar and New, 2002; Yong *et al.*, 2008). The most well-known algorithms are image fusion with additive wavelet decomposition (Gonzalez and Woods, 2002; Nunez *et al.*, 1999; Pajares and Manuel de la Cruz, 2004) and image fusion with DT-CWT (Hill *et al.*, 2002). (Yang *et al.*, 2008) proposed a medical image fusion method that is based on multiscale geometric analysis of contourlet transform. Multiscale geometric analysis was introduced by (Toet *et al.*, 1989) as contrast decomposition scheme that used to relate the luminance processing in the early stages of the human visual system. In this method the local energy was adopted for coefficient selection in the lowpass and region based contourlet contrast was adopted for highpass subband, which can preserve more details in source images and further improve the quality of fused image. The actual fusion process can take place at different levels of information representation. A common categorization is to distinguish between pixel, feature and decision level (Pohl and Van Genderen, 1998). Medical image fusion usually employs the pixel level fusion techniques. The advantage of pixel fusion is that the images use to contain the original information. Furthermore, the algorithms are rather easy to implement and time efficient.

Medical image fusion has been used to derive useful information from multimodality medical image data. This chapter presents a dual-tree complex contourlet transform (DT-CCT) based approach for the fusion of magnetic resonance image (MRI) and computed tomography (CT) images. The objective of the fusion of an MRI image and a CT image of the same organ is to obtain a single image containing as much information as possible about that organ for diagnosis. The limitation of directional information of dual-tree complex wavelet (DT-CWT) is rectified in DT-CCT by incorporating directional filter banks (DFB) into the DT-CWT. To improve the fused image quality, new methods for fusion rules which depend on frequency component of DT-CCT coefficients (contourlet domain) have been presented in this chapter.

For low frequency coefficients PCA and local energy weighted selection are incorporated as the fusion rules in a contourlet domain and for high frequency coefficients, the salient features are picked up based on local energy. The final fusion image is obtained by directly applying inverse dual tree complex contourlet transform (IDT-CCT) to the fused low and high frequency coefficients.

As the clinical use of different medical imaging systems extends, the multimodality imaging acting an increasingly important part in a medical imaging field. Different medical imaging techniques may provide scans with complementary and occasionally unnecessary information. The combination of medical images can often lead to additional clinical information not noticeable in the separate images. MRI-CT image fusion presents an accurate tool for planning the correct surgical procedure and is a benefit for the operational results in computer assisted navigated neurosurgery of temporal bone tumors (Nemec *et al.*, 2007).

2. Overview of image fusion

The goal of image fusion is to integrate complementary information from multimodality images so that the new images are more suitable for the purpose of human visual perception and computer processing. Therefore, the task of image fusion is to make many salient features in the new image such as regions and their boundaries.

Image fusion consists of putting together information coming from different modality of medical images, whereas registration consists of computing the geometrical transformation between two data sets. This geometrical transformation is used to resample one image data set to match other. An excellent registration is set for an excellent fusion. The process of information fusion can be seen as an information transfer problem in which two or more information sets are combined into a new one that should contain all the information from the original sets. During the process of fusion, input images A and B are combined into a new fused image F by transferring, ideally all of their information into F . This is illustrated graphically using a simple Venn diagram (Carroll *et al.*, 2007) in Figure 1.

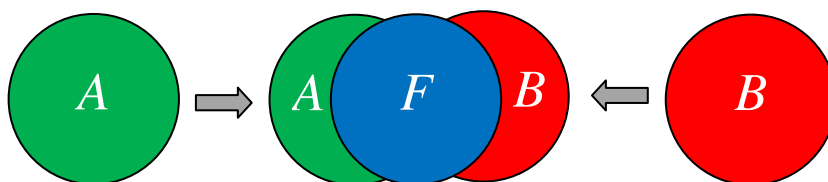


Fig. 1. Graphical representation of the image information fusion process.

The combination of images from different modalities leads to additional clinical information which is not apparent in the separate imaging modality. For this reason radiologists prefer multiple imaging modalities to obtain more details. Image fusion is performed to extract all the useful information from the individual modality and integrate them into one image. In general, a successful fusion should extract complete information from source images into the result, without introducing any artifacts or inconsistencies.

Medical image fusion usually employs the pixel level fusion techniques. The purpose of pixel-level image fusion is to represent the visual information present in input images, in a single fused image without the introduction of distortion or loss of information. The advantage of pixel level fusion is that the images used the contained the original information. Furthermore, the algorithms are rather easy to implement and time efficient. The classification of pixel-to-pixel based image fusion methods is illustrated in Figure 2. The aim of this classification was to identify, with different degrees of detail, complexity and accuracy. The main component is the domain of implemented the image fusion which however are not always strictly separable (Chen and Li, 2005). Many algorithms developed so far can be classified into four primary categories:

1. Substitution methods such as principal component analysis (PCA) (Ghassemian, 2001), averaging weighted, color mixed RGB (Baum *et al.*, 2008) and intensity hue saturation (IHS) (Ghassemian, 2001).
2. Mathematical combination which normalizes multispectral bands used for an RGB display such as Brovey Transform (Pohl and Van Genderen, 1998).
3. Optimization approach such as Bayesian and neural network (Lai and Fang, 2000).
4. Transform domain such as multiresolution decomposition which introduces spatial features from the high-resolution images into the multispectral images. For example, Laplacian pyramid (Burt, 1984), wavelets (Zhang and Hong, 2005), curvelet (Ali *et al.*, 2008), contourlet transform (Zheng *et al.*, 2007) and Nonsampled contourlet transform (Cunha *et al.*, 2006; Zhang and Guo, 2009).

Primitive fusion schemes based on substitution methods, such as averaging, weighted averaging and PCA, are performed solely in the substitution domain. In spite of easy implementation, these methods pay the expenses of reducing the contrast and distorting the spectral characteristics (Piella, 2003). Image fusion based on multiresolution decomposition (MRD) can handle the contrast and overall intensity. It decomposes images at a different scale to several components, which account for important salient features of images (Piella, 2003). Therefore, it enables a better performance than those performed in the substitution methods. The transform domain or multiresolution fusion have been discussed widely in recent studies because of their advantages over the other fusion techniques (Ali *et al.*, 2008; Mandal *et al.*, 2009; Nemeč *et al.*, 2007; Piella, 2003; Zheng *et al.*, 2007). On the other hand, methods utilized Bayesian optimization, neural network or Brovey transform to find the fused image are suffered from a significant increase of computational complexity (Pohl and Van Genderen, 1998; Byeungwoo and Landgrebe, 1999). Bayesian fusion method has been proposed, allowing to adaptively estimating the relationships between the multiple image sensors in order to generate a single enhanced display (Lai and Fang, 2000).

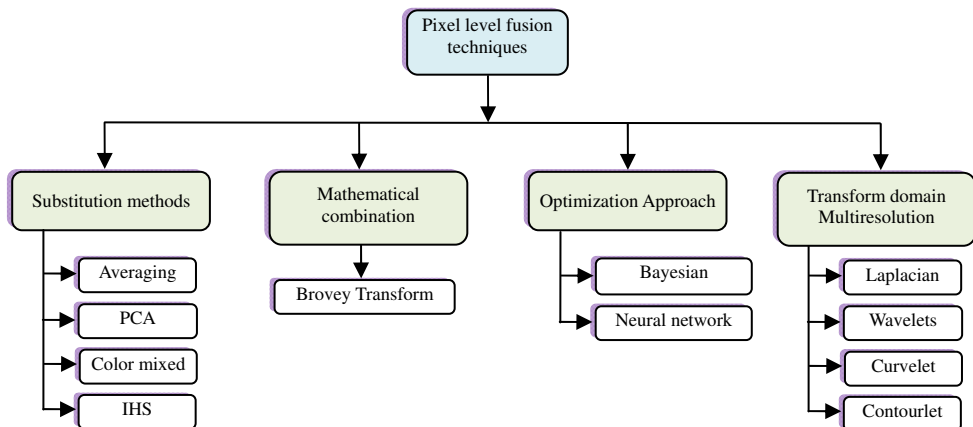


Fig. 2. The classification of pixel-to-pixel based image fusion methods.

The first multiresolution image fusion approach proposed in the literature is due to (Burt, 1984). His implementation used the Laplacian pyramid and the sample-based maximum selection rule. In (Toet, 1989) presented a similar algorithm but using the ratio of low pass pyramid. His approach is motivated by the fact that the human visual system is based on contrast, and therefore, a fusion technique which selects the highest local luminance contrast is likely to provide better details to a human observer. Several transforms have been proposed for image signals, which have incorporated directionality and multiresolution and hence, could capture edges in natural images more efficiently (Ali *et al.*, 2008; Mandal *et al.*, 2009; Nemeč *et al.*, 2007; Zheng *et al.*, 2007).

3. Dual tree complex contourlet transform

A complex contourlet transform (CCT) method is proposed by (Chen and Li, 2005), which incorporates the DT-CWT (Hill *et al.*, 2002) and DFB to provide a flexible and robust scale-

direction representation for source images. The DT-CWT decomposition details space W_j at the J -th scale, gives six subbands at each scale capturing distinct directions. Traditionally, we obtain the three highpass bands corresponding to the LH, HL, and HH subbands, indexed by $i \in \{1, 2, 3\}$. Each of them has two wavelets as real and complex part. By averaging the outputs of dual tree, we get an approximate of shift invariant (Kingsbury, 1999). In second stage for each subband applied (l_j) levels DFB (Bamberger and Smith, 1992) as shown in Figure 3. W_j of DT-CWT is nearly shift invariant and this property can be still established in the subspace $W_{j,k}^{(l_j)}$, even after applying directional filter banks on a detail subspace W_j . The mathematical form is defined as:

$$\eta_{j,k,n}^{i,(l_j)} = \sum_{m \in \mathbb{Z}^2} g_k^{l_j}[m - S_k^{(l_j)}n] \psi_{j,m}^i \quad i = 1, 2, 3 \tag{1}$$

where $g_k^{(l)}$ is the impulse response of the synthesis filter, $S_k^{(l)}$ is overall downsampling matrices of DFB and ψ is a wavelet functions. The family $\{\eta_{j,k,n}^{HL,(l_j)}, \eta_{j,k,n}^{LH,(l_j)}, \eta_{j,k,n}^{HH,(l_j)}\}_{n \in \mathbb{Z}^2}$ is a basis for the subspace $W_{j,k}^{(l_j)}$ and each consists of a complex dual tree. The location shift is denoted as m .

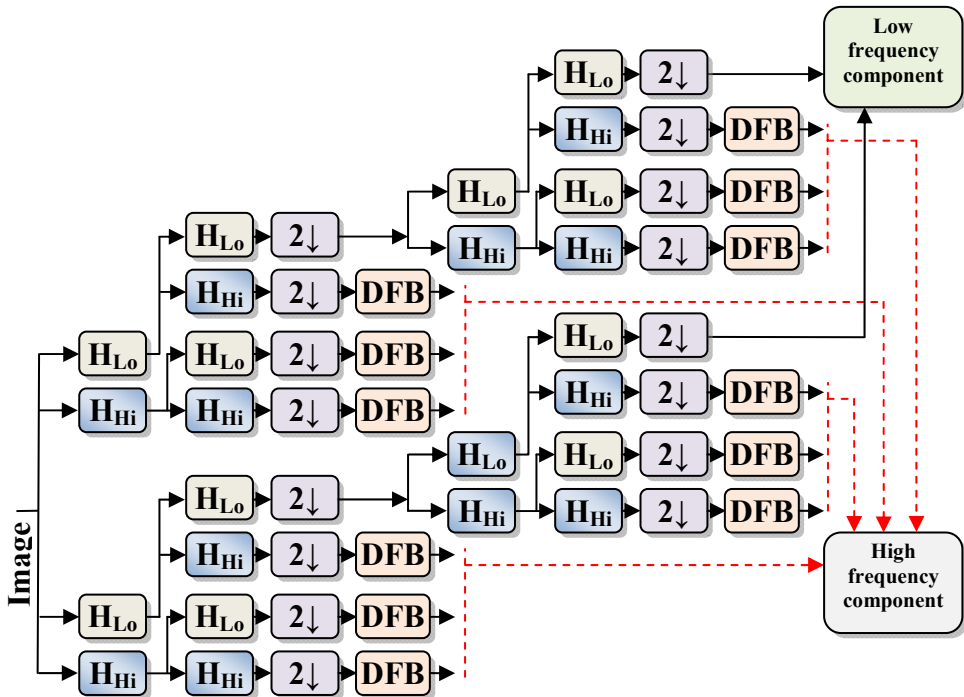


Fig. 3. The proposed of DT-CCT based on Fusion Rules.

3.1 Requirements and challenges of image fusion

The reason of image fusion is to integrate complementary and redundant information from multiple images to produce a combined that contains a superior description of the scene than any of the individual source images. Considering the objectives of image fusion and its potential advantages, some generic requirements can be imposed on the fusion algorithm (Rockinger, 1996):

- It should not discard any salient information contained in any of the input images.
- It should not introduce any artifacts which can distract or mislead a human observer or any subsequent image processing steps.
- It must be reliable, robust and, as much as possible, tolerant of imperfections such as noise or misregistrations.

However, a fusion approach which is independent of the modalities of the inputs and produces a combined image which appears accepted to a human interpreter is highly wanted.

3.2 Image fusion approach (DT-CCT-PCA and DT-CCT-PCA/LE)

The proposed image fusion approach consists of the following steps:

- Step 1.** Perform a DT-CCT on source images A and B , respectively, and obtain the corresponding coefficients $\{\text{Coff}_{j,l}^{(L,A)}, \text{Coff}_{j,l}^{(H,A)}\}$ and $\{\text{Coff}_{j,l}^{(L,B)}, \text{Coff}_{j,l}^{(H,B)}\}$, where $\text{Coff}_{j,l}^{(L,A)}$ and $\text{Coff}_{j,l}^{(L,B)}$ represent low frequency coefficients of image A and B respectively at the coarsest scale. $\text{Coff}_{j,l}^{(H,A)}$ and $\text{Coff}_{j,l}^{(H,B)}$ denotes the high frequency coefficients of image A and B respectively at the J -th scale and the l -th direction of DFP.
- Step 2.** Employ some fusion rules to reconstruct the DT-CCT coefficients of the fused image F as shown $\{\text{Coff}_{j,l}^{(L,F)}, \text{Coff}_{j,l}^{(H,F)}\}$.
- Step 3.** By successively performing inverse dual tree complex contourlet transform to the modified coefficients at all decomposition, the final fused image F can be reconstructed.

3.2.1 Fusion rules for low frequency coefficients

The following are the methods proposed for fusion rules:

Method 1: Complex contourlet transform based on maximum selection (CCT-Max)

As the coefficients in the coarsest scale subband $\{\text{Coff}_{j_0}^{(L,A \text{ or } B)}\}$ represents the approximation component of the source image, the simplest way is to use the conventional maximum selection method to produce the composite coefficients. The maximum selection method is a popular choice to pick out the salient features of an image, e.g. edges and boundaries.

The normalized weight $D^{(L,A)} \in \{0,1\}$ is defined as:

$$D^{(L,A)} = \begin{cases} 1 & \left| \text{Coff}_{j_0}^{(L,A)} \right| \geq \left| \text{Coff}_{j_0}^{(L,B)} \right| \\ 0 & \text{otherwise} \end{cases} \quad (2)$$

where $D^{(L,A)}$ and $D^{(L,B)} = 1 - D^{(L,A)}$ are used in equation (7) to obtain the coefficients of low frequency coefficients for fused image. This method were used in CCT-Max proposed by (Chen and Li, 2005). However, it cannot obtain fused approximation of high quality for medical image.

Method 2: Dual tree complex contourlet transform based on PCA (DT-CCT-PCA)

The principal component analysis PCA can be used as a weighted precision measure to determine which pixel or region is important for fused. Dual tree complex contourlet transform based on PCA is implemented as described in (Al-Azzawi *et al.*, 2009; Al-Azzawi and Abdullah, 2010). PCA is also called the Karhunen-Loève transform or the Hotelling transform. It involves a mathematical procedure that transforms a number of correlated variables into a number of uncorrelated variables called principal components. It is also used to reduce dimensionality in a dataset while retaining those characteristics of the dataset that contribute most to its variance. It computes a compact and optimal description of the data set. PCA has been employed in previous researches (Huaixin, 2007; Zheng *et al.*, 2005) as fusion rules. The fusion rule for low frequency component in contourlet domain is implemented as:

$$D^{(L,A)} = \frac{i}{i+j} \quad \text{and} \quad D^{(L,B)} = \frac{j}{i+j} \tag{3}$$

where i and j are the elements of the principal eigenvector, which are computed by analyzing the original input image A and B for corresponding image coefficients. $D^{(L,A)}$ and $D^{(L,B)}$ are the normalized weights. Thus the fused image has the same energy distribution as the original input images.

Method 3: Dual tree complex contourlet transform based on PCA and Local energy (DT-CCT-PCA/LE).

In this method, PCA and local energy weighted selection are incorporated as the fusion rules in contourlet domain. First, calculate the local energy $E^{(A \text{ or } B)}_{Low}(x,y)$ of low frequency component in contourlet domain centering at the current coefficient $Coff_{j_0}^{(L,A \text{ or } B)}$ (Nunez *et al.*, 1999; Pudney *et al.*, 1995), which is defined as:

$$E^{(A \text{ or } B)}_{Low}(x,y)_{j_0} = \sum_m \sum_n Coff_{j_0}^{(L,A \text{ or } B)}(x+m,y+n)^2 \cdot W(m,n) \tag{4}$$

where W is a template of size 3×3 and satisfy the normalization rule.

$$W = \frac{1}{9} \begin{bmatrix} 1 & 1 & 1 \\ 1 & 1 & 1 \\ 1 & 1 & 1 \end{bmatrix} \quad \text{and} \quad \sum_m \sum_n W(m,n) = 1 \tag{5}$$

The normalized weight $D^{(L,A \text{ or } B)} \in \{0,1\}$ is defined as:

$$\left\{ \begin{array}{l} D^{(L,A)} = \begin{cases} 1 & |E^{(A)}_{Low}(x,y)_{j_0}| \geq |E^{(B)}_{Low}(x,y)_{j_0}| \\ 0 & \text{otherwise} \end{cases} \\ D^{(L,B)} = 1 - D^{(L,A)} \end{array} \right\} \quad \text{for } E^{(A \text{ or } B)}_{Low}(x,y)_{j_0} \geq \partial \tag{6}$$

$$\left\{ \begin{array}{l} D^{(L,A)} = i / (i + j) \\ D^{(L,B)} = j / (i + j) \end{array} \right\} \quad \text{for } E^{(A \text{ or } B)}_{Low}(x,y)_{j_0} < \partial$$

where i and j are the elements of the principal eigenvector, which are computed by analyzing the original input image A and B for corresponding image coefficients. ϑ is threshold defined by user. $D^{(L,A)}$ and $D^{(L,B)}$ are the normalized weights. The coefficients of low frequency components for fused image F is shown below:

$$\text{Coff}_{j_0}^{(L,F)} = \text{Coff}_{j_0}^{(L,A)} \cdot D^{(L,A)} + \text{Coff}_{j_0}^{(L,B)} \cdot D^{(L,B)} \quad (7)$$

3.2.2 Fusion rules for high frequency coefficients

High frequency coefficients generally correspond to sharper brightness in the image. The most commonly used selection principle is the local energy scheme to pick out the salient features of an image, e.g. edges and boundaries. The local energy (Yang *et al.*, 2008; Morrone and Owens, 1987) $E^{(A)}_{\text{High}}(x,y)$ and $E^{(B)}_{\text{High}}(x,y)$ is defined as:

$$E^{(A \text{ or } B)}_{\text{High}}(x,y)_{j,l} = \sum_m \sum_n \text{Coff}_{j,l}^{(H,A \text{ or } B)}(x+m,y+n)^2 \cdot W(m,n) \quad (8)$$

where W is a template defined in equation (5). Larger value of local energy $E^{(A \text{ or } B)}_{\text{High}}(x,y)$ means there is more high frequency information. Weights $D^{(H,A)}$ and $D^{(H,B)}$ needs to be calculated as:

$$D^{(H,A)} = \begin{cases} 1 & \text{for } E^{(A)}_{\text{High}}(x,y) \geq E^{(B)}_{\text{High}}(x,y) \\ 0 & \text{for } E^{(A)}_{\text{High}}(x,y) < E^{(B)}_{\text{High}}(x,y) \end{cases} \text{ and } D^{(H,B)} = 1 - D^{(H,A)} \quad (9)$$

The coefficients of high frequency coefficients for fused image F is defined as:

$$\text{Coff}_{j,l}^{(H,F)} = \text{Coff}_{j,l}^{(H,A)} \cdot D^{(H,A)} + \text{Coff}_{j,l}^{(H,B)} \cdot D^{(H,B)} \quad (10)$$

The multiresolution coefficients with large local energy values are considered as sharp brightness changes or salient features in the corresponding source image, such as the edges, lines, contours and object boundaries. So, the fused high frequency components in contourlet domain preserve all the salient features in source images and introduce as less artifacts or inconsistency as possible. Therefore, the fusion result will contain all high resolution form original image.

4. Objective evaluation of image fusion

Objective evaluations of fused images are important in comparing the performance of different image fusion algorithms (Petrovic and Xydeas, 2005a; Petrovic and Xydeas, 2005b; Ruiz *et al.*, 2002; Yinghua *et al.*, 2007; Youzhi and Zheng, 2009). Objective evaluation methods are needed to compare "good" or "bad" fused images. So far, only a limited number of relatively application dependent objective image fusion performance metrics has been published in the literature (Petrovic and Xydeas, 2005b; Piella, 2003; Wang and Bovik,

2002; Yang *et al.*, 2008; Rockinger and Fechner, 1998). Many image quality evaluations in the literature use an ideal fused image as a reference for comparison with the image fusion results (Yinghua *et al.*, 2007; Li *et al.*, 1995). Rockinger and Fechner, (1998) proposed metrics based on mutual information for image sequence and still image fusion performance.

The root mean squared error and peak signal to noise ratio-based metrics were widely used for these comparisons. The gradient representation metric of (Petrovic and Xydeas, 2005b) is based on the idea of measuring localized preservation of input gradient information in the fused image. An image quality index based on the structural metric proposed by (Wang and Bovik, 2002) was improved for image fusion assessment by (Piella and Heijmans, 2003) into a pixel by pixel or region by region method, giving weighted averages of the similarities between the fused image and each of the source images.

A reliable method for choosing an optimal fusion algorithm for each particular application however, largely remains an open issue. A number of objective comparison metrics have been investigated:

Image Quality Index (IQI), is easy to calculate and applicable to various image processing application (Wang and Bovik, 2002; Piella and Heijmans, 2003). The dynamic range of IQI is [-1, 1]. The best value 1 is achieved if and only if $F = R$, where F is fused image and R is reference image. IQI is defined as:

$$IQI = \frac{\sigma_{FR}}{\sigma_F \sigma_R} \cdot \frac{2\overline{FR}}{(\overline{F})^2 + (\overline{R})^2} \cdot \frac{2\sigma_F \sigma_R}{\sigma_F^2 + \sigma_R^2} \tag{11}$$

where :

$$\overline{g} = \frac{1}{Z} \sum_{i=1}^Z g_i, \sigma_{FR} = \frac{1}{Z-1} \sum_{i=1}^Z (F_i - \overline{F})(R_i - \overline{R}) \text{ and } \sigma_g^2 = \frac{1}{Z-1} \sum_{i=1}^Z (g_i - \overline{g})^2,$$

$$g = F \text{ or } R \text{ and } Z = N \times M \text{ (size of the image).}$$

Coefficient Correlation (CC), can show similarity in the small structures between the original and reconstructed images (Roche *et al.*, 1998). Higher value of correlation means that more information is preserved. Coefficient correlation in the space domain is defined by:

$$d = \text{image A or image B.}$$

$$CC(F, d) = \frac{\sum_{i=0}^{M-1} \sum_{j=0}^{N-1} (F(i, j) - \overline{F})(d(i, j) - \overline{d})}{\sqrt{\sum_{i=0}^{M-1} \sum_{j=0}^{N-1} (F(i, j) - \overline{F})^2 \sum_{i=0}^{M-1} \sum_{j=0}^{N-1} (d(i, j) - \overline{d})^2}} \tag{12}$$

where \overline{F} and \overline{d} are the mean value of the corresponding data set.

Overall Cross Entropy (OCE), is used to measure the difference between the two source images and the fused image. Small value corresponds to good fusion result obtained (Yang *et al.*, 2008). The OCE calculation is as follows:

$$\text{OCE}(A,B;F) = \frac{CE(A,F) + CE(B,F)}{2} \quad (13)$$

where $CE(A,F)$ and $CE(B,F)$ are the cross entropy of the source image and fused image respectively, given by following:

$$CE(d,F) = \sum_{i=0}^{L-1} p_d(i) \log_2 \frac{p_d(i)}{p_f(i)} \quad (14)$$

where $d = A$ or B is the input multimodality medical images, F is the fused image result, p_f , p_d are the normalized histogram of the fused image and source image respectively, and L is the maximum gray level for a pixel in the image, usually L is set to 255.

Root Mean Square Error (RMSE), is found between the reference image R and the fused image F , (Zheng *et al.*, 2005), defined as:

$$\text{RMSE} = \left(\frac{1}{c}\right) \sum_k \sqrt{\frac{\sum_{x=1}^N \sum_{y=1}^M (R_k(x,y) - F_k(x,y))^2}{M \times N}} \quad (15)$$

where $c=3$ and $k=R,G,B$ for color image and $c=1$ for gray image. The smaller the value of the RMSE means a better performance of the fusion algorithm.

5. Experimental results for image fusion

In this section, we present some experimental results obtained with presented fusion methods.

5.1 Robust image fusion using Dual Tree Complex Contourlet Transform (DT-CCT-PCA and DT-CCT-PCA/LE)

To test proposed method, thirty five groups of human brain images were selected, includes a CT and a MRI images. The corresponding pixels of two input images have been perfectly co-aligned. All images have the same size of 512×512 pixels, with 256-level grayscale. The proposed medical fusion algorithm, traditional complex contourlet and DT-CWT are applied to these image sets. In our experiment an image is decomposed into 2-levels using biorthogonal Daubechies 9-7 wavelet, (Lina and Gagnon, 1995; Mallat, 1999).

Each subband at each level is fed to the DFB stage with 8-directions at the finest level. In the DFB stage, the 23-45 biorthogonal quincunx filters were used designed by (See-May *et al.*, 1995) and modulate them to obtain the biorthogonal fan filters. DT-CWT is available in Matlab wavelet software (Selesnick *et al.*, 2003).

In addition, image quality index (IQI), root mean square error (RMSE), correlation coefficient (CC) and overall cross entropy (OCE) are used to evaluate the fusion performance (objective evaluation). Experiment results were conducted to compare the proposed methods DT-CCT-PCA and DT-CCT-PCA/LE with complex contourlet transform based on maximum amplitudes (CCT-max) (Chen and Li, 2005) and dual tree complex

wavelet transform (DT-DWT) (Hill *et al.*, 2002). Figure 4, it shows the original multimodality image dataset 1 and 2.

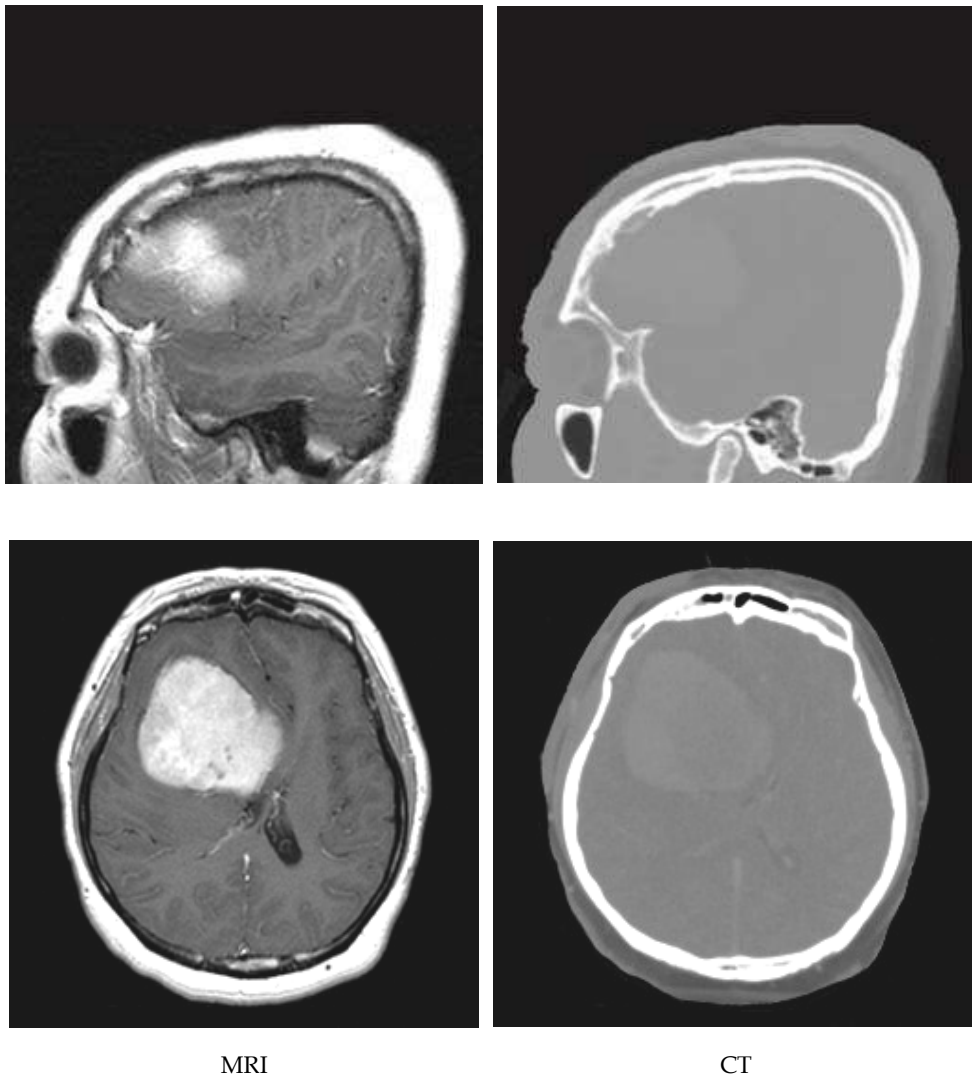


Fig. 4. Original multimodality image dataset 1 and 2.

The evaluation results in Table 1 and the complete data sets show that:

1. From indicators, the IQI and CC are the best with the proposed methods, higher value of correlation or IQI, means that more information is preserved. The OCE and RMSE of the new methods are least in the two sets. It is shown that, the proposed method gives the best fusion results in the two fused images.

2. For the two image sets, the corresponding fused image results are given in Figure 5. DT-CCT-PCA performs better than previous method. However, the best image fusion result is obtained by applying the proposed DT-CCT-PCA/LE fusion algorithm.
3. It is evident to see from the Table 1 and the complete data sets that the resulting image from DT-CCT-PCA/LE based fusion has better spectral quality than the other methods, in terms of the higher values of correlation coefficient and root mean square error. The highest value of correlation coefficient 0.9929 in this case indicates that most geometric details are enhanced in the image fused by DT-CCT-PCA/LE transform. As it could be seen from the preceding experimental results, DT-CCT-PCA/LE based fusion approach is the optimum and most well-suited fusion MRI-CT application, in terms of the spectral and spatial quality.
4. Fusion scheme based the novel weighted PCA/LE rule can get better fusion image. As shown in Table 1 and the complete data sets, for DT-CCT-PCA/LE the RMSE and OCE are both lower than that of traditional based methods, lowest values of RMSE and OCE are 0.1017, 0.4527 respectively. The lowest values of RMSE and OCE are 0.1683, 0.8726 respectively for CCT-max.
5. Experimental results demonstrate that the proposed method DT-CCT-PCA/LE outperforms the DT-CCT-PCA-based fusion approach and the traditional CCT-max-based approaches and including the DT-CWT-based in terms of both visual quality and objective evaluation.

Data	Evaluation	DT-CWT	CCT-max	DT-CCT-PCA	DT-CCT-PCA/LE
Data set 1	IQI	0.2581	0.2513	0.3236	0.4250
	RMSE	0.1683	0.1683	0.1442	0.1017
	CC	0.9482	0.9482	0.9523	0.9641
	OCE	0.8726	0.8726	0.8683	0.8531
Data set 2	IQI	0.3340	0.3523	0.4171	0.3843
	RMSE	0.2179	0.2180	0.1480	0.2281
	CC	0.9750	0.9750	0.9853	0.9929
	OCE	1.0865	1.0863	0.9911	0.4527

Table 1. Results of Quality Measures for Various Fusion Schemes.

6. Conclusion

A new approach for multimodal image fusion using dual-tree complex contourlet transform (DT-CCT) based on PCA and combined (PCA and local energy) are proposed. The method is based on PCA, local energy and dual tree complex contourlet transform. We can see from Figure 5 that the feature and detailed information presented in section 3.2.1 method 3 is much richer than other fused images. The image contents like tissues are clearly enhanced. Other useful information like brain boundaries and shape are almost perfectly. The dual tree complex contourlet transform produces images with improved contours and textures, while the property of shift invariance is retained. It enhances the reliability of conventional approaches considerably and thereby their acceptability by practitioners in a clinical environment.

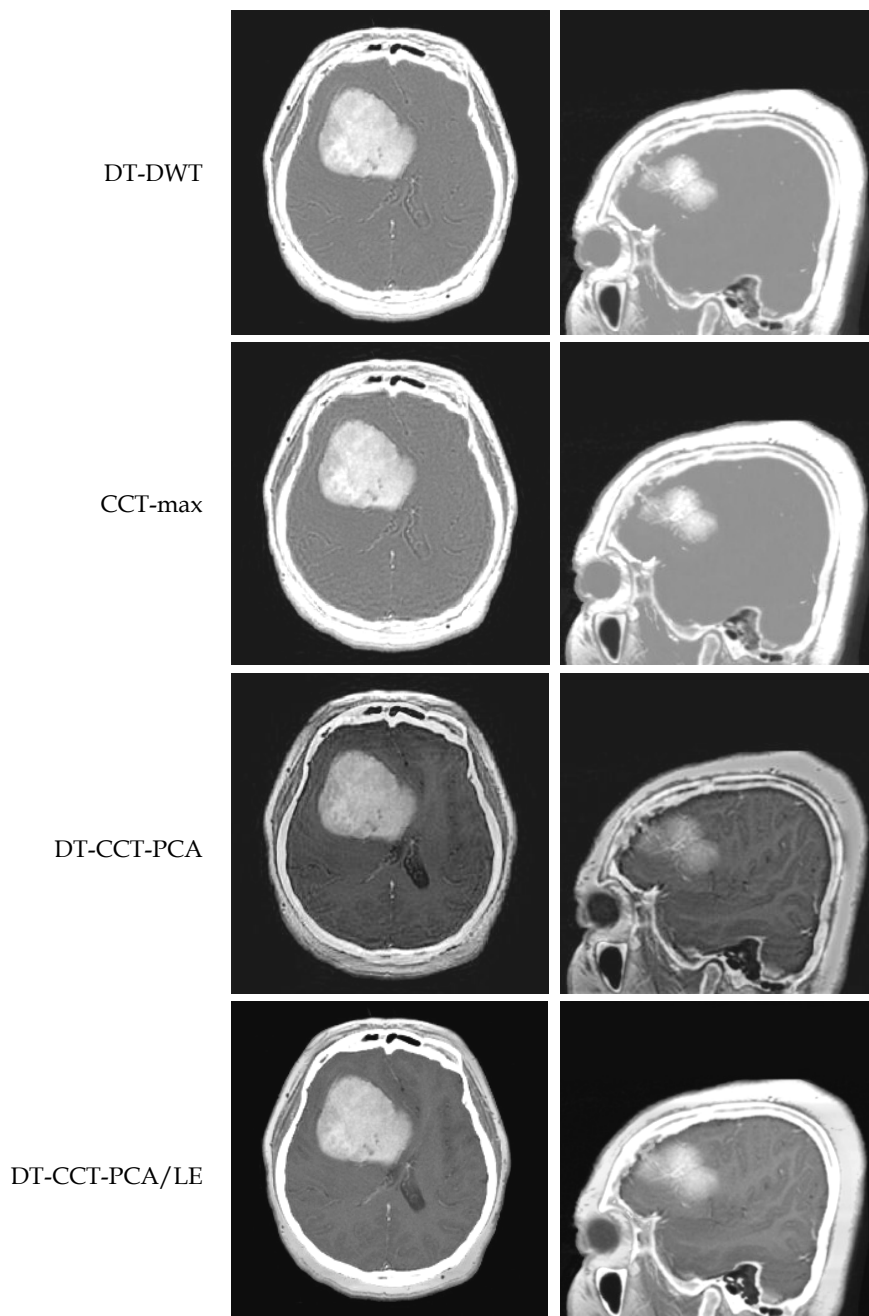


Fig. 5. Fusion results on test original multimodality image dataset 1 and 2 using DT-CWT, traditional CCT-max and proposed methods.

The methods present a new development in the fusion of MRI and CT images, which is based on the DT-CCT. Visual and objective evaluation comparisons demonstrated that the fusion results (Figure 5) of the new method contain more detail information, while information distortion is very small. It enhances the reliability of conventional approaches considerably and thereby their acceptability by practitioners in a clinical environment.

7. Acknowledgment

Authors of this chapter sincerely would like to thank Hospital Universiti Sains Malaysia (HUSM) for provided all medical images.

8. References

- Aguilar, M. & New, J. R. (2002). Fusion of multi-modality volumetric medical imagery, *In Proceedings of the Fifth International Conference on Information Fusion*, 2, pp. 1206-1212, ISBN 0-9721844-1-4, Annapolis, MD, 2002.
- Al-Azzawi, N., Sakim, H. A. M., Abdullah, W. A. K. W. & Ibrahim, H. (2009). Medical image fusion scheme using complex contourlet transform based on PCA, *Annual International Conference of the IEEE Engineering in Medicine and Biology Society, EMBC 2009*, pp. 5813-5816, ISBN 1557-170X, Hilton Minneapolis, Minnesota, USA, 2-6 September, 2009.
- Al-Azzawi, N. A. & Abdullah, W. A. K. W. (2010). Improved CT-MR image fusion scheme using dual tree complex contourlet transform based on PCA. *International Journal of Information Acquisition*, Vol. 7, No.2, pp. 99-107, ISSN 0219-8789.
- Ali, F. E., El-Dokany, I. M., Saad, A. A. & El-Samie, F. E. A. (2008). Curvelet fusion of MR and CT images. *Progress In Electromagnetics Research C*, Vol. 3, pp. 215-224, ISSN 1937-8718.
- Anna, W., Wu, L., Li, D. & Chen, Y. (2007). Research on medical image fusion based on orthogonal wavelet packets transformation combined with 2v-SVM, *IEEE/ICME International Conference on Complex Medical Engineering*, pp. 670-675, ISBN 978-1-4244-1078-1, Beijing, 23-27 May, 2007.
- Bamberger, R. H. & Smith, M. J. T. (1992). A filter bank for the directional decomposition of images: Theory and design. *IEEE Transactions on Signal Processing*, Vol. 40, No.4, pp. 882-893, ISSN 1053587X.
- Baum, K., Helguera, M. & Krol, A. (2008). Fusion viewer: A new tool for fusion and visualization of multimodal medical data sets. *Journal of Digital Imaging*, Vol. 21, pp. 59-68, ISSN 0897-1889.
- Burt, P. (1984). The pyramid as a structure for efficient computation, *Multiresolution Image Processing and Analysis*, A. Rosenfeld, Ed. Springer-Verlag, Berlin, pp. 6-35, ISBN 0387130063, 1984.
- Byeungwoo, J. & Landgrebe, D. A. (1999). Decision fusion approach for multitemporal classification. *IEEE Transactions on Geoscience and Remote Sensing*, Vol. 37, No.3, pp. 1227-1233, ISSN 0196-2892.

- Carroll, J., Ruskey, F. & Weston, M. (2007). Which n-venn diagrams can be drawn with convex k-gons? *Discrete and Computational Geometry*, Vol. 37, No.4, pp. 619-628, ISSN 0179-5376.
- Chen, D. & Li, Q. (2005). The use of complex contourlet transform on fusion scheme. *proceedings of world academy of science, engineering and technology*, Vol. 7, pp. 342-347, ISSN 975-98458-6-5.
- Cunha, A. L. D., Zhou, J. P. & Do, M. N. (2006). The nonsampled contourlet transform: theory, design, and applications. *IEEE Transactions on Image Processing*, Vol. 15, No.10, pp. 3089-3101, ISSN 1057-7149.
- Daneshvar, S. & Ghassemian, H. (2007). Fusion of MRI and PET images using retina based multi-resolution transforms, *9th International Symposium on Signal Processing and its Applications, ISSPA 2007*, pp. 1-4, ISBN 978-1-4244-0778-1, Sharjah, United arab emirates, 12-15 February, 2007.
- Ghassemian, H. (2001). A retina based multi-resolution image-fusion, *IEEE International Geoscience and Remote Sensing Symposium. IGARSS '01*, 2, pp. 709-711, ISBN 0-7803-7031-7, Sydney, NSW, 9-13 July, 2001.
- Gonzalez, R. C. & Woods, R. E. (2002). *Digital image processing*. (Second Edition), Prentice Hall, ISBN 0201180758, Upper Saddle River, N.J.
- Hill, P. R., Canagarajah, C. N. & Bull, D. R. (2002). Image fusion using complex wavelets, *Electronic Proceedings of 13th British Machine Vision Conference, BMVC 02*, pp. 487-496, ISBN 1 901725 19 7, Wales, 2-5 September, 2002.
- Hong, Z., Lei, L. & Nan, L. (2007). A novel wavelet medical image fusion method, *International Conference on Multimedia and Ubiquitous Engineering, MUE '07*, pp. 548-553, ISBN 0-7695-2777-9, Seoul, 26-28 April, 2007.
- Huaixin, C. (2007). A multiresolution image fusion based on principle component analysis, *Fourth International Conference on Image and Graphics, ICIG 2007*, pp. 737-741, ISBN 0-7695-2929-1, Sichuan, 22-24 August, 2007.
- Kingsbury, N. (1999). Shift invariant properties of the dual-tree complex wavelet transform, *Proceedings IEEE International Conference on Acoustics, Speech, and Signal Processing, ICASSP '99*, 3, pp. 1221-1224, ISBN 0-7803-5041-3, Phoenix, AZ., 15-19 March, 1999.
- Lai, S.-H. & Fang, M. (2000). A hierarchical neural network algorithm for robust and automatic windowing of MR images. *Artificial Intelligence in Medicine*, Vol. 19, No.2, pp. 97-119, ISSN 0933-3657.
- Li, H., Manjunath, B. S. & Mitra, S. K. (1995). Multisensor image fusion using the wavelet transform. *Graphical Models and Image Processing*, Vol. 57, No.3, pp. 235-245, ISSN 1077-3169.
- Lina, J.-M. & Gagnon, L. (1995). Image enhancement with symmetric Daubechies wavelets, *Wavelet Applications in Signal and Image Processing III. Part 1 (of 2)*, Society of Photo-Optical Instrumentation Engineers, 2569, pp. 196-207, ISBN 0277786X, San Diego, CA, USA, 12-14 July, 1995.
- Mallat, S. (1999). *A wavelet tour of signal processing*. (Second Edition), Academic, ISBN 012466606X, San Diego, Calif.

- Mandal, T., Jonathan Wu, Q. M. & Yuan, Y. (2009). Curvelet based face recognition via dimension reduction. *Signal Processing*, Vol. 89, No.12, pp. 2345-2353, ISSN 0165-1684.
- Morrone, M. C. & Owens, R. A. (1987). Feature detection from local energy. *Pattern Recognition Letters*, Vol. 6, No.5, pp. 303-313, ISSN 0167-8655.
- Nemec, S. F., Donat, M. A., Mehraïn, S., Friedrich, K., Krestan, C., Matula, C., Imhof, H. & Czerny, C. (2007). CT-MR image data fusion for computer assisted navigated neurosurgery of temporal bone tumors. *European Journal of Radiology*, Vol. 62, No.2, pp. 192-198, ISSN 0720-048X.
- Nunez, J., Otazu, X., Fors, O., Prades, A., Pala, V. & Arbiol, R. (1999). Multiresolution-based image fusion with additive wavelet decomposition. *IEEE Transactions on Geoscience and Remote Sensing*, Vol. 37, No.3, pp. 1204-1211, ISSN 0196-2892.
- Pajares, G. & Manuel De La Cruz, J. (2004). A wavelet-based image fusion tutorial. *Pattern Recognition*, Vol. 37, No.9, pp. 1855-1872, ISSN 0031-3203.
- Patias, P. (2002). Medical imaging challenges photogrammetry. *ISPRS Journal of Photogrammetry and Remote Sensing*, Vol. 56, No.5-6, pp. 295-310, ISSN 0924-2716.
- Petrovic, V. & Xydeas, C. (2005a). Objective evaluation of signal-level image fusion performance. *Optical Engineering*, Vol. 14, No.8, pp. 1-8, ISSN 00913286.
- Petrovic, V. & Xydeas, C. (2005b). Objective image fusion performance characterisation, *Tenth IEEE International Conference on Computer Vision, ICCV 2005*, 2, pp. 1866-1871, ISBN 1550-5499, Beijing, 17-21 October, 2005b.
- Piella, G. (2003). A general framework for multiresolution image fusion: from pixels to regions. *Information Fusion*, Vol. 4, No.4, pp. 259-280, ISSN 1566-2535.
- Piella, G. & Heijmans, H. (2003). A new quality metric for image fusion, *Proceedings International Conference on Image Processing, ICIP 2003*, 3, pp. 173-176, ISBN 1522-4880, Barcelona Catalonia, Spain, 14-17 September, 2003.
- Pohl, C. & Van Genderen, J. L. (1998). Multisensor image fusion in remote sensing: concepts, methods and applications. *International Journal of Remote Sensing*, Vol. 19, No.5, pp. 823-854, ISSN 01431161.
- Pudney, C., Kovesi, P. & Robbins, B. (1995). A 3D local energy surface detector for confocal microscope images, *Proceedings of the Third Australian and New Zealand Conference on Intelligent Information Systems, ANZIIS-95*, pp. 7-12, ISBN 0-86422-430-3, Perth, WA, Australia, 27 November, 1995.
- Roche, A., Malandain, G., Pennec, X. & Ayache, N. (1998). The correlation ratio as a new similarity measure for multimodal image registration. In: WELLS, W. M., COLCHESTER, A. & DELP, S. (eds.) *Medical Image Computing and Computer-Assisted Intervention - MICCAI'98*. Springer Berlin Heidelberg, 1496, pp. 1115-1124, ISBN 978-3-540-65136-9.
- Rockinger, O. (1996). Pixel-level fusion of image sequences using wavelet frames, In *Proceedings of the 16th Leeds Annual Statistical Research Workshop, LASR1996*, Leeds University Press, pp. 149-154, ISBN 0853161615, Leeds, England, July, 1996.
- Rockinger, O. & Fechner, T. (1998). Pixel-Level Image Fusion: The Case of Image Sequences, *SPIE proceedings series, Signal processing, sensor fusion, and target recognition VII*, 3374, pp. 378-388, ISBN 0-8194-2823-X, Orlando FL, ETATS-UNIS, 1998.

- Ruiz, V. G., Fernández, J. J., López, M. F. & García, I. (2002). Progressive image transmission in telemicroscopy: A quantitative approach for electron microscopy images of biological specimens. *Real-Time Imaging*, Vol. 8, No.6, pp. 519-544, ISSN 1077-2014.
- See-May, P., Kim, C. W., Vaidyanathan, P. P. & Ansari, R. (1995). A new class of two-channel biorthogonal filter banks and wavelet bases. *IEEE Transactions on Signal Processing*, Vol. 43, No.3, pp. 649-665, ISSN 1053-587X.
- Selesnick, I., Cai, S. & Li, K. (2003). *Matlab implementation of wavelet transforms*. January 2008. Available from: <http://taco.poly.edu/WaveletSoftware/index.html>.
- Singh, R., Vatsa, M. & Noore, A. (2009). Multimodal medical image fusion using redundant discrete wavelet transform, *Seventh International Conference on Advances in Pattern Recognition, ICAPR '09*, pp. 232-235, ISBN 978-1-4244-3335-3, Kolkata, 4-6 February, 2009.
- Toet, A. (1989). Image fusion by a ratio of low-pass pyramid. *Pattern Recognition Letters*, Vol. 9, No.4, pp. 245-253, ISSN 0167-8655.
- Toet, A., Ruyven, L. V. & Velaton, J. (1989). Merging thermal and visual images by a contrast pyramid. *Optical Engineering*, Vol. 28, No.7, pp. 789-792, ISSN 0091-3286.
- Wang, Z. & Bovik, A. C. (2002). A universal image quality index. *IEEE Signal Processing Letters*, Vol. 9, No.3, pp. 81-84, ISSN 10709908.
- Yang, L., Guo, B. L. & Ni, W. (2008). Multimodality medical image fusion based on multiscale geometric analysis of contourlet transform. *Neurocomputing*, Vol. 72, No.1-3, pp. 203-211, ISSN 0925-2312.
- Yinghua, L., Xue, F., Jingbo, Z., Rujuan, W., Kaiyuan, Z. & Jun, K. (2007). A multi-focus image fusion based on wavelet and region detection, *The International Conference on 'Computer as a Tool', EUROCON, 2007, 3*, pp. 294-298., ISBN 978-1-4244-0813-9, Warsaw, Poland, 9-12 September, 2007.
- Yong, C., You, H. & Chaolong, Y. (2008). CT and MRI image fusion based on contourlet using a novel rule, *The 2nd International Conference on Bioinformatics and Biomedical Engineering, ICBBE 2008*, pp. 2064-2067, ISBN 978-1-4244-1747-6, Shanghai, 16-18 May, 2008.
- Youzhi, Z. & Zheng, Q. (2009). Objective image fusion quality evaluation using structural similarity. *Tsinghua Science and Technology*, Vol. 14, No.6, pp. 703-709, ISSN 1007-0214.
- Zhang, Q. & Guo, B.-L. (2009). Multifocus image fusion using the nonsubsampled contourlet transform. *Signal Processing*, Vol. 89, No.7, pp. 1334-1346, ISSN 0165-1684.
- Zhang, Y. & Hong, G. (2005). An IHS and wavelet integrated approach to improve pan-sharpening visual quality of natural colour IKONOS and QuickBird images. *Information Fusion*, Vol. 6, No.3, pp. 225-234, ISSN 1566-2535.
- Zheng, Y., Essock, E. A. & Hansen, B. C. (2005). Advanced discrete wavelet transform fusion algorithm and its optimization by using the metric of image quality index. *Optical Engineering*, Vol. 44, No.3, pp. 037003(1-12), ISSN 0091-3286.
- Zheng, Y., Song, J. S., Zhou, W. M. & Wang, R. H. (2007). False color fusion for multi-band SAR images based on contourlet transform. *Acta Automatica Sinica*, Vol. 33, No.4, pp. 337-341, ISSN 1874-1029.

Zhongfei, Z., Jian, Y., Bajwa, S. & Gudas, T. (2003). "Automatic" multimodal medical image fusion, *Proceedings. 16th IEEE Symposium on Computer-Based Medical Systems*, pp. 42-49, ISBN 0-7695-1901-6, New York, NY, USA, 26-27 June, 2003.

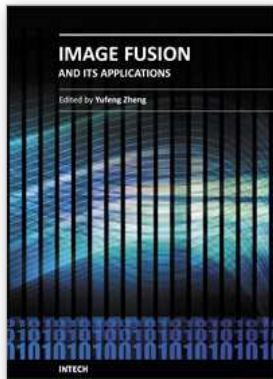


Image Fusion and Its Applications

Edited by Dr. Yufeng Zheng

ISBN 978-953-307-182-4

Hard cover, 242 pages

Publisher InTech

Published online 24, June, 2011

Published in print edition June, 2011

The purpose of this book is to provide an overview of basic image fusion techniques and serve as an introduction to image fusion applications in variant fields. It is anticipated that it will be useful for research scientists to capture recent developments and to spark new ideas within the image fusion domain. With an emphasis on both the basic and advanced applications of image fusion, this 12-chapter book covers a number of unique concepts that have been graphically represented throughout to enhance readability, such as the wavelet-based image fusion introduced in chapter 2 and the 3D fusion that is proposed in Chapter 5. The remainder of the book focuses on the area application-orientated image fusions, which cover the areas of medical applications, remote sensing and GIS, material analysis, face detection, and plant water stress analysis.

How to reference

In order to correctly reference this scholarly work, feel free to copy and paste the following:

Nemir Al-Azzawi and Wan Ahmed K. Wan Abdullah (2011). Medical Image Fusion Schemes Using Contourlet Transform and PCA Bases, Image Fusion and Its Applications, Dr. Yufeng Zheng (Ed.), ISBN: 978-953-307-182-4, InTech, Available from: <http://www.intechopen.com/books/image-fusion-and-its-applications/medical-image-fusion-schemes-using-contourlet-transform-and-pca-bases>

INTECH

open science | open minds

InTech Europe

University Campus STeP Ri
Slavka Krautzeka 83/A
51000 Rijeka, Croatia
Phone: +385 (51) 770 447
Fax: +385 (51) 686 166
www.intechopen.com

InTech China

Unit 405, Office Block, Hotel Equatorial Shanghai
No.65, Yan An Road (West), Shanghai, 200040, China
中国上海市延安西路65号上海国际贵都大饭店办公楼405单元
Phone: +86-21-62489820
Fax: +86-21-62489821

© 2011 The Author(s). Licensee IntechOpen. This chapter is distributed under the terms of the [Creative Commons Attribution-NonCommercial-ShareAlike-3.0 License](#), which permits use, distribution and reproduction for non-commercial purposes, provided the original is properly cited and derivative works building on this content are distributed under the same license.